Addiction Biology

WILEY

Addiction Biology SSA

ORIGINAL ARTICLE OPEN ACCESS

Structural Cerebellar and Lateral Frontoparietal Networks are altered in CUD: An SBM Analysis

Elena Lacomba-Arnau[1,2] | Agustín Martínez-Molina[3] | Alfonso Barrós-Loscertales[4]

[1]Departament de Psicologia, Sociologia i Treball Social, Universitat de Lleida, Lleida, Spain | [2]Department of Precision Health, Luxembourg Institute of Health, Strassen, Luxembourg | [3]Departamento de Psicología Social y Metodología, Universidad Autónoma de Madrid, Madrid, Spain | [4]Departament de Psicologia Bàsica, Clínica i Psicobiologia, Universitat Jaume I, Castellón, Spain

Correspondence: Elena Lacomba-Arnau (elacomba@uji.es) | Alfonso Barrós-Loscertales (barros@uji.es)

Received: 8 July 2024 | **Revised:** 14 January 2025 | **Accepted:** 20 January 2025

Funding: The publication is part of the project PID2021-127340NB-C21, funded by Ministerio de Ciencia e Innovación (MCIN/AEI/10.13039/501100011033/FEDER, EU); participation of EL-A was supported by a grant of the Agència de Gestió d'Ajuts Universitaris i de Recerca de la Generalitat de Catalunya (2023 FI-3 00107) and a grant of Universidad Autónoma de Madrid (CA5/RSUE/2022-00133) to AMM.

Keywords: Addiction | Cocaine Use Disorder | Independent Component Analysis | Source-based Morphometry | Structural Networks

ABSTRACT

Repetitive drug use results in enduring structural and functional changes in the brain. Addiction research has consistently revealed significant modifications in key brain networks related to reward, habit, salience, executive function, memory and self-regulation. Techniques like Voxel-based Morphometry have highlighted large-scale structural differences in grey matter across distinct groups. Source-based Morphometry (SBM) takes this a step further by incorporating the Independent Component Analysis to detect shared patterns of grey matter variation, all without requiring prior selection of regions of interest. However, SBM has yet to be employed in the study of structural alteration patterns related to cocaine addiction. Therefore, we performed this analysis to explore alterations in structural covariance specific to cocaine addiction. Our study involved 40 individuals diagnosed with Cocaine Use Disorder (CUD) and 40 matched healthy controls. Participants with CUD completed clinical questionnaires assessing the severity of their dependence and other relevant clinical variables. Following the adjustment for age-related effects, we observed notable disparities between groups in two structural independent components, which we identified as the structural cerebellar network and the structural lateral frontoparietal network, which display opposing trends. Specifically, the individuals with CUD exhibited a heightened contribution to the cerebellar network but simultaneously demonstrated a reduced contribution to the lateral frontoparietal network compared to the healthy controls. These findings unveil distinctive covariance patterns of neuroregulation linked with cocaine addiction, which indicates an interruption in the typical structural development in an affected lateral frontoparietal network, while suggesting an extended pattern of neuroregulation within the cerebellar network in individuals with CUD.

1 | Introduction

Neuroimaging research is widely used to explore structural and functional alterations associated with Cocaine Use Disorder (CUD). Repetitive drug use leads to brain changes until drug-taking transforms into habit [1]. Structural alterations associated with cocaine dependence have shown to be spread along cortical and subcortical areas [2–4]. These morphometric adaptations have been associated with several self-report and clinical variables, such as age of onset and duration [5–10, 15], severity of dependence [3, 11] and treatment status [2, 7, 12]. Current neurobiological models of addiction argue that part of the symptomatology present in substance use disorder is a consequence of a new neural organisation, which

leads to changes in the circuits involved with reward, memory, motivation, executive function, mood and interoception [4, 13–19]. Therefore, neurobiological theories of addiction and empirical research lead to the prediction of changes in structural networks.

Voxel-based Morphometry (VBM) studies have been used to show macrostructural alterations in the brain's grey matter of patients with CUD. These differences are widespread when considered across studies [2, 20, 21]. MRI studies have demonstrated that the human brain is organised into complex structural and functional networks [22–25]. However, brain networks are not static but instead fluctuate [26–29]. When studying pathologies, the instability of functional networks could be confusing [30]. The structural methodology offers applications with more accurate and stable results than functional methods [31–34]. It is also known that brain areas whose volumes covary together could be reflecting functional connectivity [35].

Source-based Morphometry (SBM) is an extension of VBM [36], which includes a principal component analysis followed by an Independent Component Analysis (ICA) blockset [37, 38]. The SBM tool is applied to identify sources of grey matter variation and to perform a statistical analysis to identify which sources distinguish patients from healthy controls (HCs) [38–40]. As the SBM considers interrelations across different voxels, its application allows patterns of structural covariance to be identified [40]. Furthermore, whereas univariate approaches link data based on the correlation done separately for each point, multivariate approaches like ICA focus on links between patterns by preserving spatial correlation between different brain regions [41, 42] and capturing covariations of the grey matter morphology, which is commonly used to detect local shape changes [43]. Identifying patterns of structural covariation between different brain areas while preserving spatial correlation allows these patterns to be characterised in terms of brain networks.

At the same time, the analysis of the relations between multiple variables that characterise SBM captures complex interactions between different brain regions, which allows these relations to be compared between groups [44]. This renders this tool advantageous over other techniques when studying any pathology [35]. Moreover, unlike voxel or Region-of-interest (ROI)–based techniques, SBM does not require any *a priori* selection of regions to analyse and acts as a spatial filter to separate signals that overlap and present different behaviours (e.g. artefacts vs. real brain changes) [35]. Given its advantages over other techniques, SBM has been recently applied to study several brain-related disorders. Group comparisons between controls and patients have successfully revealed differences in grey matter concentration (GMc) in studies of epilepsy [45], bipolar disorder [46, 47], schizophrenia [48–50], autism spectrum [51], Parkinson's disease [52, 53], multiple sclerosis [54], Huntington's disease [55] and individuals arrested for violent crimes [56], as mostly reviewed by Gupta, Turner, and Calhoun [35]. Indeed, the usefulness of the ICA in the functional identification of neural circuits involved in cocaine addiction has already been observed [16, 17, 19, 57].

Drug use has been associated with multiple brain impairments, some of which are common across different substances, while others are unique to specific drugs [3, 9, 15]. Shared effects include reduced volume with use in the right anterior cingulate cortex, left putamen and left insula, as well as increased volume in the left putamen [3]. On the other hand, cocaine-dependent individuals exhibit exclusive structural impairments in the supramarginal gyrus, left inferior parietal cortex and insula [58]. Previous CUD studies also report grey matter reductions in several regions, including the right hippocampus, right middle temporal gyrus, right inferior frontal gyrus [3, 21], right insula, left superior frontal gyrus [21], left putamen and left nucleus accumbens [59]. Additionally, there is an increased grey matter volume (GMv) in the caudate and orbitofrontal cortex among cocaine users [60] and an enlarged striatal volume [61]. In line with this, previous functional studies have reported alterations in CUD in the limbic, ventral frontostriatal, dorsal attentional and executive networks [2, 7, 19, 62–68]. However, as far as we know, the SBM technique has not yet been applied to study addiction and very little is known about morphological covariance network alterations in CUD.

In this study, we perform SBM to investigate alterations in the MRI structural covariance at the whole brain level and to explore the structural networks associated with cocaine addiction through this data-driven approach. We specifically applied an ICA through the SBM technique to identify patterns of common GMc variation altered in CUD and to study the link of those patterns with clinical and self-report information on addiction severity. In agreement with previous reports of brain alterations in CUD, we expected to find altered structural covariance involving target networks, such as frontostriatal, limbic, executive and cerebellar networks. We also expected these patterns of altered structural covariance in CUD patients to be linked with clinical and self-report information.

2 | Materials and Methods

2.1 | Samples

Eighty males were studied: 40 CUD patients and 40 HCs. Groups were matched by age and educational level (see Table 1). In addition, as seen in Table 1, we did not find any significant differences in total intracranial volume ($t = -0.072$, $p = 0.942$). HC participants were recruited through advertising posters and word of mouth. No HC had major medical

TABLE 1 | Sociodemographic data.

	Healthy controls ($N = 40$)	CUD patients ($N = 40$)	*t*-value HCs vs. CUD	*p* value
Age	35.45 (9.01) *20–56*	35.70 (7.56) *21–53*	0.134	0.893
IC	10.40 (2.15)	9.49 (3)	−1.56	0.124
TIV	1536.69 (113.98)	1534.89 (107.74)	−0.072	0.942

Note: The first two columns show the mean, standard deviation (in brackets) and range (in italics) of variables.
Abbreviations: CUD: cocaine use disorder patients; HCs: healthy controls; IC: intellectual coefficient; TIV: total intracranial volume.

illnesses, DSM-IV Axis I disorders or a history of head injury with loss of consciousness. CUD patients were recruited at the Addictive Behaviors Unit of Castellón (Spain) from among those who recently visited the clinic to manage their abstinence. An interview, which included the structured clinical interview for DSM-IV Axis I disorders, ensured that all the patients met the DSM-IV criteria for cocaine dependence. The Unit includes continued abstinence monitoring with random urine toxicology testing or clinical interviews held with a psychiatrist lasting 2/4 days prior to MRI acquisition. None of these patients met the criteria for either current or previous dependence of drugs other than cocaine. According to the Edinburgh Handedness Inventory [69, 70], the HCs sample was composed of 2.5% ($n = 1$) left-handed, while the CUD patients' sample comprised 10% ($n = 4$) left-handed and 5% ($n = 2$) ambidextrous when considering one missing datum in the CUD group. All the CUD and HC participants had already participated in three of any of the prior fMRI studies [16, 17, 65]. However, this was the first time that we explored differences in brain morphometry by means of SBM. As far as we know, this is the first time that an SBM analysis of cocaine addiction is reported. Before participating in this study, all the individuals were presented with detailed information about the research purpose, and they all provided written informed consent. Additionally, participants received compensation for their involvement. The study was approved by the institutional review board of the Universitat Jaume I of Castellón.

2.2 | Clinical Measures

We evaluated cocaine addiction severity using the Spanish version of the Severity Dependence Scale (SDS; [71]), the Cocaine Selective Severity Assessment (CSSA; [72]) and the Cocaine Craving Questionnaire (CCQ-B and CCQ-G; [73]). Finally, clinical history variables such as the age of onset of cocaine use, years of cocaine use and maximum abstinence period (in months) were recorded for further analyses. See Table 2 for more details.

TABLE 2 | Clinical features of CUD patient sample.

	Patients	N (max. 40)
Total Cocaine Craving Questionnaire (CCQ-B) score	14.35 (6.52)	40
Total Cocaine Craving Questionnaire (CCQ-G) score	39.79 (18.19)	39
Total Severity Dependence Scale (SDS) score	8.28 (3.19)	39
Total Cocaine Selective Severity Assessment (CSSA) score	16.77 (18.71)	39
Age of onset	19.31 (3.52)	39
Years of cocaine use	12.97 (6.91)	39
Abstinence period	14.55 (19.92)	39

Note: The first column shows the mean and standard deviation (in brackets).

2.3 | Data Acquisition and Preprocessing

Whole-brain 3D images were all acquired with the same 1.5-T Siemens Avanto scanner (Erlangen, Germany). A high-resolution structural T1-weighted MPRAGE sequence was acquired (TE, 3.8 ms; TR, 2200 ms; flip angle, 15°; matrix, $256 \times 256 \times 160$ mm; voxel size, 1 mm^3). VBM was performed with the CAT12 toolbox (version 12.6, r1450; [74]) for SPM12 (version 7487; Wellcome Department of Imaging Neuroscience, London, United Kingdom). The preprocessing pipeline of the original images followed the standard CAT12 manual recommendations (http://www.neuro.uni-jena.de/cat/). This included (a) segmentation of images into grey matter (GM), white matter and cerebrospinal fluid; (b) registration to a standard template provided by the ICBM; (c) DARTEL normalisation of the GM segments to the Montreal Neurological Institute (MNI) template; and (d) modulation by the linear and nonlinear components derived from spatial normalisation. Spatial smoothing was applied to unmodulated images using a Gaussian kernel with a full width at half maximum (FWHM) of 8 mm to enhance the signal-to-noise ratio and to facilitate group comparisons. After preprocessing, a data quality check was carried out by analysing sample homogeneity using covariance. No outliers were identified. At this point, images were ready to be analysed by SBM. Unmodulated/GMc images were used for the SBM analysis because they have been the preferred choice in seminal SBM studies [38, 40]. GMc images offer robust, spatially consistent results [75, 76] and demonstrate higher replication reliability patterns [48, 75, 76] compared to modulated/GMv images. Additionally, GMc images enable the detection of subtle structural variations without the confounding effects of volume-related differences introduced by the multiplication of Jacobian determinants during normalisation. Although these determinants are essential for modulated/GMv images, they can increase within-group variance and reduce statistical power [38]. For between-group contrasts, modulated/GMv images were used by leveraging the previously extracted components from the SBM analysis.

2.4 | SBM Analysis

The SBM algorithm was applied to identify patterns of common variation of grey matter across both groups: CUD patients and HCs. SBM is a feature identification technique used in neuroimaging research [77]. Its application allows covariance networks to be identified [38] while preserving the spatial correlation between different brain regions [41, 42]. Moreover, unlike voxel- or ROI-based techniques, SBM eliminates the need for *a priori* selection of regions for analysis and serves as a spatial filter to differentiate signals that overlap and exhibit different characteristics (e.g. artefacts vs. actual brain changes; [35]).

After the previously described preprocessing steps, the SBM analysis was implemented using the GIFT toolbox [78] on GMc images. An ICA was applied to break up the mixed signal that came from all the images for the purpose to maximally recognise spatially independent sources. This step was

applied on the GMc images using the Group ICA of fMRI Toolbox to perform SBM [35, 38]. The Infomax algorithm was selected to maximise the recognition of independent components (ICs) from GMc images' signal information [79, 80]. Then, the ICASSO algorithm was chosen [81] to study the reliability of the ICA algorithm (RandInit mode), and the ICA was run 100 times.

The ICA decomposes GMc into maximally independent GMc spatial or component maps. Each component represents a different pattern of covariation between voxels among subjects. Therefore, each voxel represents its own contribution to the underlying source for each component, or *vice versa*. The matrix returned by the ICA software during the analysis was an $n \times m$ matrix, where n represents the number of subjects (in rows) and m represents the number of ICs extracted (in columns). The subject loading coefficients returned in the matrix represent the contribution or weight of each IC to the GMc for each subject included in the study. Thus, each value determines how each component was expressed in each subject [82]. Later, we performed statistical analyses to examine any significantly different sources between both the CUD patients and HCs groups. Finally, spatial coordinates and the volume of specific covariation patterns were extracted using the Mango software [83].

2.5 | Feature Identification

Following the SBM methodology recommendation [38, 84, 85], we extracted 20 structural Independent Components (s-ICs) for the posterior comparison between samples. All the 20 s-ICs were inspected through the stability index (Iq) to ensure great stability in component decomposition. Afterward, all the 20 s-ICs were visually inspected by two reviewers and the grey matter composition of each component was evaluated. We excluded three s-ICs with a poor stability index ($Iq < 0.90$) and one s-IC with a significant spatial overlap with ventricles (the s-IC 15). Finally, 16 s-IC met the inclusion criteria for further analyses.

2.6 | Statistical Analyses

Structural network differences between the CUD and HC groups were tested using a two-sample independent t-test. Next, we ran a MANCOVA on those s-IC SBM coefficients that showed significant differences between groups in order to take into account the association between both components and regressing out age effects, following Gupta, Turner and Calhoun's [35] recommendations. A threshold of $p < 0.05$ corrected for multiple testing by the false discovery rate (FDR) method [86] was applied to find a significant effect of group and age on s-IC [35].

To describe the relations between the different s-ICs, we performed partial correlations *(two-tailed)* among the s-IC loading parameters by controlling the age effect [87]. Partial correlations were specifically explored between the s-ICs that were significantly different between groups and the other components that were not significant. Likewise, the relation between the s-IC loading parameters and the clinical and self-report information regarding addiction severity (described in Table 2) was also studied by performing partial correlations and controlling the age effect.

After identifying significant differences between groups in s-IC2 and s-IC17, a mask of each s-IC was created using the Mango software to estimate statistical differences in GMv in these components. The full component image was loaded without applying any additional z-threshold or statistical filtering to ensure that all clusters in the component were included for the analysis (e.g. s-IC2 included 24 clusters and s-IC17 included 85 clusters). The z-value range for s-IC2 went from 3 to 9 and from 2 to 6 for s-IC17, as derived directly from the ICA loading coefficients. Using the MNI atlas as a spatial reference, we identified overlapping clusters in each s-IC following the next steps: (1) a mask was generated for each s-IC using the Mango software by loading the full positive component image (see Figure 2); (2) each s-IC mask was overlapped with the MNI atlas to identify the spatial extent of the overlap and to determine the regions corresponding to each cluster; and (3) the extent of the volume covered by each s-IC was calculated by summarising the voxel volumes from GMv maps for all clusters identified in the component. However, only the statistical details of the eight largest clusters, representing the most prominent overlaps between the s-IC mask and MNI atlas regions, are presented. These statistics are provided in the supplementary table (Table S1), which summarises the global and point statistics including mean z-scores, sum, SD, size (mm^3), maximum z-value, and corresponding coordinates (X, Y, Z) for each cluster. Each individual mean s-IC component score represented the contribution of each component to a given subject [87]. This workflow was used to extract the mean structural GMv of those s-IC that showed significant differences between groups.

Next, the masks created for each s-IC from the previous workflow was used to extract the mean structural GMv of those s-ICs showing significant differences between groups. Thus, we acquired the modulated GMvs without applying smoothing from each s-IC using a MATLAB script [88], as previously applied in studies conducted by our research team [89]. Following this, we assessed the GMv distinctions between patients with CUD and HCs. Additionally, we explored any potential correlations between the volumetric characteristics of the components displaying significant group disparities and the volumetric characteristics of the remaining components. Finally, we examined the relations between s-IC volume and the clinical and self-report data concerning the addiction severity by implementing partial correlations, while controlling for age and TIV effects.

All the statistical analyses were performed with IBM SPSS 28 Statistics [90].

3 | Results

3.1 | Brain Morphometric Results

3.1.1 | s-IC Loading Parameters From GMc

A two-sample t-test *(one-tailed)* allowed us to identify which s-IC showed between-group differences in loading coefficients. Only two structural networks differed significantly

between CUD and HCs, identified as s-IC2 and s-IC17. As seen in Figures 1 and 2, s-IC2 is primarily composed of the cerebellum with some involvement of other brain regions, such as the middle frontal gyrus, the superior parietal lobe, the lentiform nucleus and the lingual gyrus. Thus, we refer to it as the CN. On the other hand, s-IC17 involves the core regions of the lateral frontoparietal network (L-FPN; [25]) and we refer to it as the L-FPN. The CN exhibited an increased GMc pattern in CUD patients compared to HCs (s-IC2; t (80) = 2.128, $p = 0.018$; $Iq > 0.98$; $d = 0.48$). In contrast, the structural L-FPN showed a decreased GMc pattern in CUD patients when compared to HCs (s-IC17; t (80) = −2.224, $p = 0.015$; $Iq > 0.92$; $d = -0.50$). In order to take into account the age effect and between-s-IC associations, a MANCOVA was performed with the SBM coefficients of GMc [35]. The results confirmed the same between-group disparities in the CN (s-IC2; F (6,052), $p = 0.016$; $\eta p2 = 0.06$) and the L-FPN (s-IC17; F (5,160), $p = 0.026$; $\eta p2 = 0.06$), as depicted in Table 3. Figures 1 and 2 illustrate these structural networks. Both differences survived FDR correction ($p < 0.05$).

The correlations between s-IC were explored and compared both across and between groups, respectively. We focused only on the correlations involving components s-IC2 and s-IC17. By exploring the relation between s-IC loading parameters, we found that some significant relations involved the structural L-FPN when using the *Fisher r-to-z transformation* to assess the significance of the difference between two correlation coefficients (using the

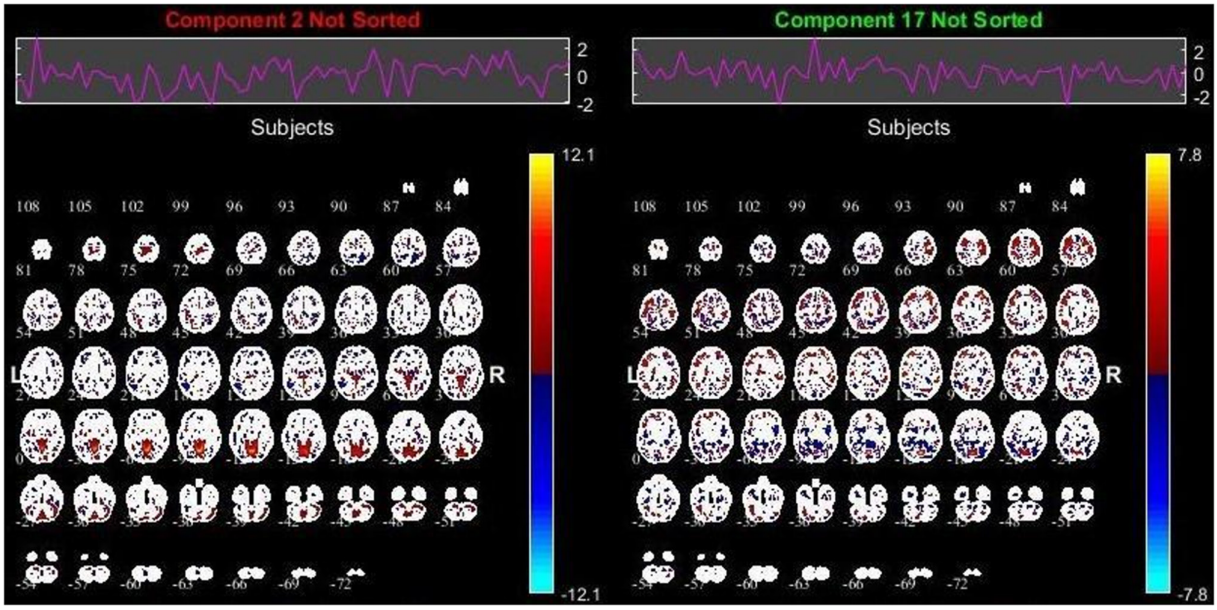

FIGURE 1 | Structural independent components showing significant differences between cocaine use disorder (CUD) and healthy controls (HCs). *Note*: on the left, the cerebellar network (s-IC2); on the right, the lateral frontoparietal network (s-IC17).

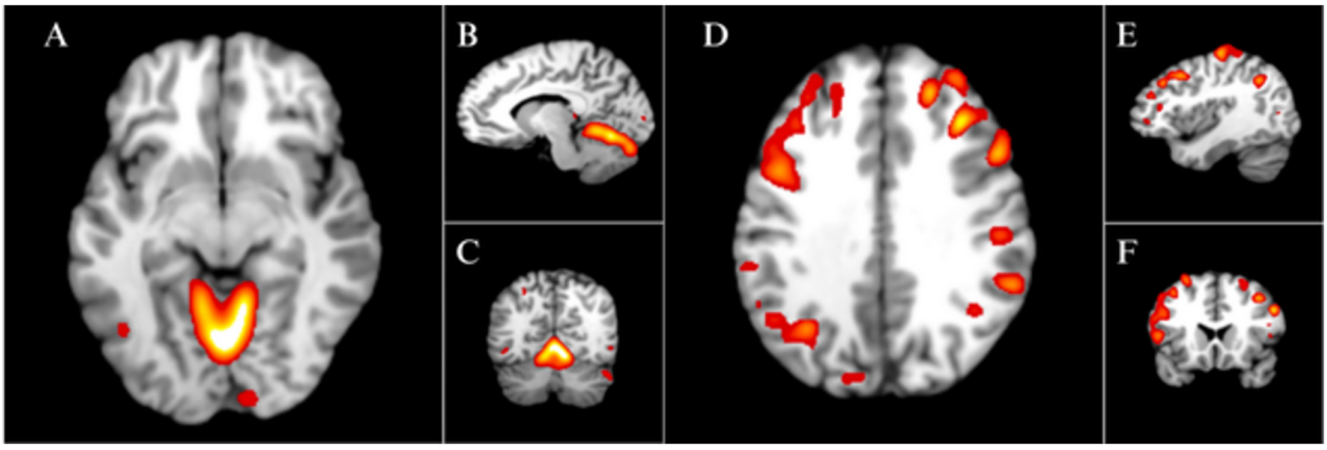

FIGURE 2 | Structural independent components showing significant differences between cocaine use disorder (CUD) and healthy controls (HCs) visualised in the Mango software. *Note*: The figure illustrates the structural independent components (s-ICs) superimposed on the MNI atlas in the Mango software. The left column represents the cerebellar network (s-IC2), and the right column represents the lateral frontoparietal network (s-IC17). Panels (A), (B) and (C) show the axial, sagittal and coronal views of s-IC2, respectively. Panels (D), (E) and (F), respectively depict the axial, sagittal and coronal views of s-IC17. These views highlight the spatial distribution of brain regions that exhibited significant differences between cocaine use disorder (CUD) and healthy controls (HCs).

TABLE 3 | Structural independent component loading parameters from grey matter concentration showing significant differences between the cocaine use disorder (CUD) patients and healthy controls (HCs).

Structural Independent Component	Brain Region Label (Atlas 3)	BA	Structural network identified	Loadings directionality	Mean (SD)	*F*	*p* value
s-IC2	Culmen of Vermis	*	Cerebellar Network	CUD > HC	0.46 (0.22)	6.052	0.016*
	Culmen	*					
	Mid Frontal Gyrus	9					
	Sup Parietal Lobe	7					
	Lentiform Nucleus	Putamen					
	Lingual Gyrus	18					
s-IC17	Declive of Vermis	*	Lateral Frontoparietal Network	CUD < HC	−0.48 (0.22)	5.16	0.026*
	Mid Frontal Gyrus	6, 9, 46					
	Precuneus	7, 39					
	Inf Parietal Lobe	40					
	Precentral Gyrus	4					

Note: The second and third columns show the main brain areas involved (middle: mid; superior: sup; inferior: inf; BA: Brodmann area). The fifth column contains the loadings directionality from the grey matter concentration for the cocaine use disorder patients (CUD) and healthy control (HC). The subsequent columns show statistical results: mean (standard deviation), *F* and *p* value.
*$p < 0.05$ (MANCOVA).

coefficients found in partial correlations by groups; see Figure 3). The relations between s-IC17 and s-IC4 ($z = -1.91$, $p = 0.028$; one-tailed), between s-IC17 and s-IC9 ($z = -2.38$, $p = 0.009$; one-tailed) and between s-IC17 and s-IC16 ($z = 2.72$, $p = 0.003$; one-tailed) were significantly different between groups when comparing CUD to HCs. As Table 4 shows, we observed an opposite pattern in correlations: the relation between s-IC17 and s-IC16 was significant only for HCs, while the relations between s-IC17 and s-IC4 and between s-IC17 and s-IC9 were significant only for CUD. Details regarding the brain regions encompassed by s-IC4, s-IC9 and s-IC16 appear in Table 5. On a global scale, when age effects were controlled through two-tailed partial correlations, we observed a significant positive correlation between s-IC2 and another s-ICs as well as between s-IC17 and other s-ICs. However, it is essential to highlight that none of these correlations evidenced significant between-group differences.

3.1.2 | GMVs

GMVs were extracted from a Regions of Interest (ROIs)-based mask for each brain map of s-IC2 and s-IC17, extracted following the workflow described in the Statistical Analyses subsection. To take into account the age and TIV effects, a MANCOVA was performed with the GMv of the CN and L-FPN. The CN (represented in Table 3 and Figure 1; s-IC2; F (6,681), $p = 0.012$; $\eta p2 = 0.08$) was significantly different between groups and survived FDR correction (at $p < 0.05$). The structural L-FPN merely showed a tendency ($p < 0.10$).

The relation between GMv networks was explored globally and depending on groups. We focused only on the correlations involving s-IC2. When exploring the relation between the GMv of s-IC maps, we found some significant relations involving the CN when using the *Fisher r-to-z transformation* to assess the significance of the difference between two correlation coefficients (using the coefficients found in partial correlations by groups). Only the relation between s-IC2 and s-IC11 ($z = -1.79$, $p = 0.0367$; one-tailed) was significantly different between groups when comparing CUD to HCs, and was significant only for CUD (see s-IC11 in Figure 2). Details regarding the brain regions encompassed by s-IC11 are found in Table 5. On a global scale, when age and TIV effects were controlled through two-tailed partial correlations, we observed a significant positive correlation between s-IC2 and another s-IC. However, it is essential to highlight that none of these correlations evidenced significant between-group differences.

3.2 | Clinical Results

When exploring the relation between the s-IC loading parameters and the clinical and questionnaire scores for addiction severity in the CUD group, partial correlations with age did not reveal any significant correlations involving components s-IC2 and s-IC17 ($p > 0.1$). In the same way, when exploring the relation between the GMv of components and the clinical and questionnaire scores for addiction severity in the CUD group, partial correlations with age and TIV did not reveal any significant correlations involving s-IC2 ($p > 0.1$).

4 | Discussion

The SBM analysis identified significant between-group differences in the loading coefficients of GMc in two s-ICs, s-IC2 and s-IC17, which we named the *Cerebellar Network* (CN) and the *Laterar Frontoparietal Network* (L-FPN), respectively. As far as we know, this is the first study to report structural covariance network alterations in CUD patients using the SBM approach. Compared to HCs, the CUD patients exhibited greater contribution to the CN, which indicates a pattern of neuroadaptations that spreads along this structural network in CUD. We also observed a lower contribution of the L-FPN structure in CUD (Table 3), which may be interpreted as an interruption in the structural integrity of this network in the patient group. In fact,

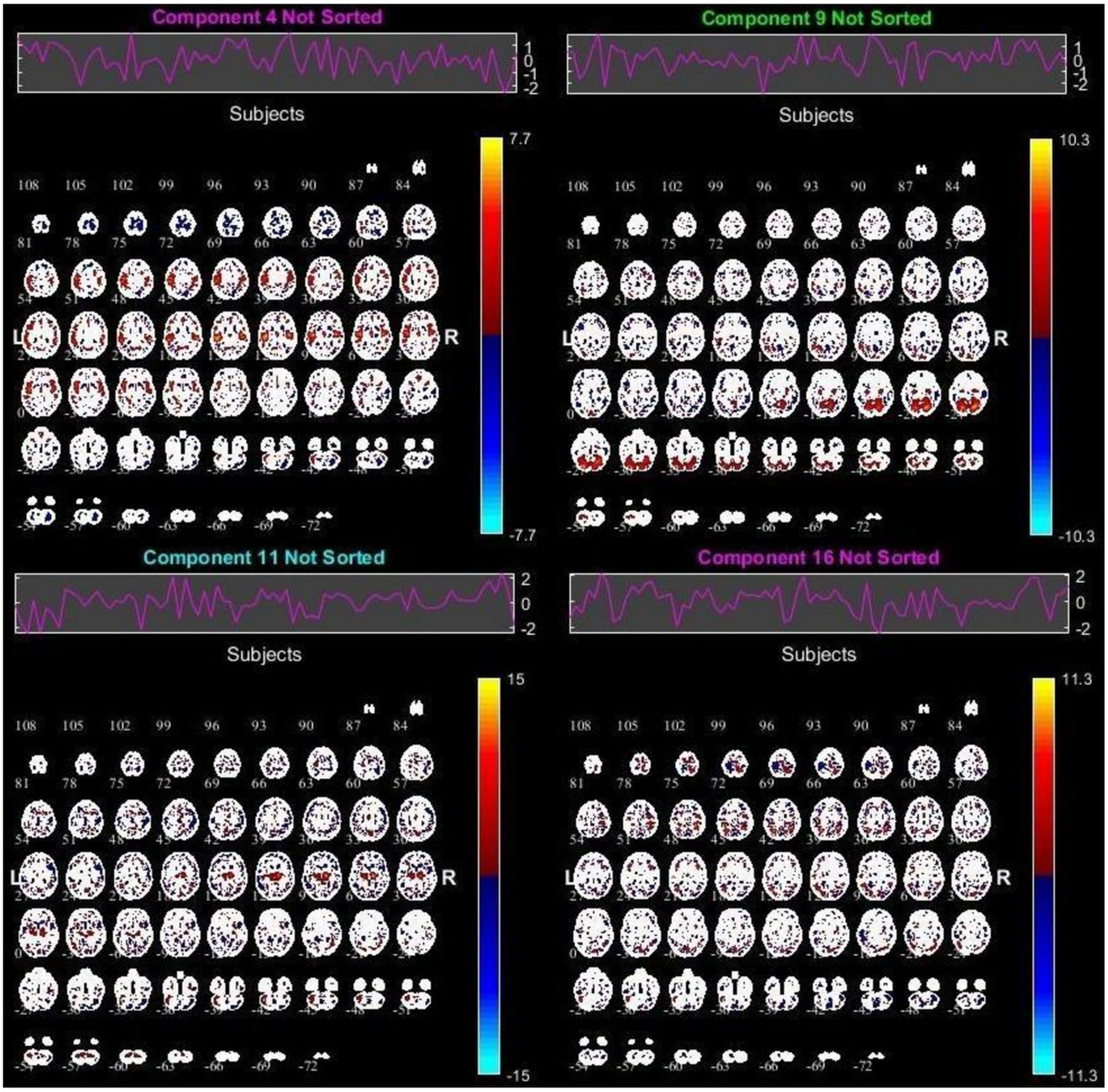

FIGURE 3 | Structural Independent Components correlated with the Structural Cerebellar Network and the Structural Frontoparietal Network. *Note:* top left, s-IC4; top right, s-IC9; bottom left, s-IC11; bottom right, s-IC16.

the structural patterns observed in the differences between groups' components may involve a disruption in the long-term functional coactivation of CUD [87, 91].

The CN primarily comprises the cerebellum, with some involvement of other brain regions previously identified in studies on cocaine users. There is a large body of MRI studies reporting structural and functional alterations in the cerebellum by cocaine addiction [5, 8, 9, 15, 92–94], although they show no clear pattern. In our study, structural covariance between the brain structures included in the CN was stronger for the CUD individuals than for HCs. This suggests significant differences in the participation of this component in the structural brain network between the two groups by reflecting a complex pattern of upregulation or facilitation of factors subserving the structural covariance driven by cocaine addiction in the CN. Therefore, the CN component may serve as a structural set of cerebellar regions, reflecting a pattern of alterations to be tested in future studies on addiction. This s-IC also included other regions, albeit to a lower extent. These other regions have shown alterations in previous studies, such as the superior parietal lobe (BA7; [95–99]), the middle frontal gyrus (BA 9; [82, 100]; as reviewed in [11, 66]), the lentiform nucleus (putamen; [11, 90, 100]) and the lingual gyrus (BA 18; [101]). These areas have been implicated in the functional alteration of psychological processes in cocaine addiction, such as inhibition [95], decision-making [98], visuospatial attention [99], working memory [96, 99], attention switching [92], cognitive control [66, 97], emotional regulation [66], craving [66], relapse [101] and impulsivity traits [11]. It is noteworthy that we observed GMv differences between groups when extracting volume values within the ROI drawn from the s-IC2 mask. In fact, we observed that CUD showed an increased GMv in the pattern of the CN component regions. This result supports our suggestion of using the CN component as a ROI in future studies, although this result may be biased given that the CN independent component was extracted from these same

TABLE 4 | Fisher coefficients of correlations between the structural independent components involving the structural cerebellar network (s-IC2) and the structural frontoparietal network (s-IC17).

	s-IC correlation	*r* coefficients for CUD patients	*r* coefficients for HC	*z* coefficient	*p* value (one-tailed)
s-IC loading parameters	s-IC17/s-IC4	−0.073	0.354	−1.91	0.028*
	s-IC17/s-IC9	−0.361	0.174	−2.38	0.009**
	s-IC17/s-IC16	0.332	−0.28	2.72	0.003**
GM volume	s-IC2/s-IC11	−0.347	0.53	−1.79	0.037*

Note: The first column shows the type of data, the second column indicates the correlation between s-IC correlations and the third and fourth columns depict the *r* coefficients for the CUD and HC groups respectively. *Z* coefficients and *p* values (one-tailed) are shown in the two last columns. In the s-IC loading parameter correlations, the age effect is controlled; in the s-IC GM volume correlations, age and TIV effects are controlled.
*$p < 0.05$.
**$p < 0.01$.

TABLE 5 | Structural component from the grey matter concentration and grey matter volumes correlating with the Cerebellar or Frontoparietal Networks.

A) Structural component loading parameters of the Structural Frontoparietal Network (s-IC17)

Structural Independent Component	Brain Region Label (Atlas 3)	BA	*Z* coefficient directionality	Group
s-IC4	Insula	13	CUD-p < HC	HC
	Cingulate Gyrus	32		
	Thalamus	Med dorsal nucleus		
	Cerebellar Tonsil	*		
	Precentral Gyrus	9		
	Inf Parietal Lobe	40		
	Post Cingulate	30		
s-IC9	Culmen	*	CUD-p < HC	CUD
	Uvula	*		
	Mid Temp Gy	39		
	Amygdala	*		
	Parahippocampus	Amygdala, 18		
	Mid Occipital Gy	*		
	Mid temporal Gy	39		
s-IC16	Angular Gyrus	39	CUD-p > HC	CUD
	Mid Temporal Gy	39		
	Declive	*		
	Postcentral Gyrus	7		
	Fusiform Gyrus	37		
	Mid Frontal Gyrus	9		
	Tuber	—		

B) GM volume of the Cerebellar Network (s-IC2)

Structural Independent Component	Brain Region Label (Atlas 3)	BA	Z coefficient directionality	Group
s-IC11	Thalamus	*, Ven pos med nuc	CUD-p < HC	CUD
	Sup Temporal Gy	39		
	Mid Temporal Gy	39		
	Precuneus	7		
	Mid Frontal Gy	6		
	Sup Parietal Lobe	7		
	Postcentral Gyrus	3		

Note: Sections A and B indicate the type of data and the network with correlates. The second and third columns contain the primary brain regions (middle: mid; superior: sup; inferior: inf; posterior: post; gyrus: gy; BA: Brodmann area). The fourth column indicates the directionality of the *z* coefficients represented in Table 3. The fifth column reveals the group in which the correlation was observed. The asterisks indicate brain regions named as such in the atlas and do not represent a level of significance.

samples, and has already shown differences in terms of individual factor scores. Indeed, the mean factor scores and the GMv values revealed a correlation across groups ($r = p < 0.001$) in a *post hoc* analysis to further explore this association. Therefore, s-IC may serve to delineate brain regional sets for multivariate analysis. Future research should determine the replicability of this CN component.

The named structural L-FPN involved mainly lateral and medial parietal regions and frontal, cerebellar and motor areas. In a previous study, Segall et al. [87] reported the structural–functional correspondence of the results of SBM-ICA analyses, in which the precuneus was shown to be a link between frontal, cerebellar, parietal and motor areas. These authors identified the precuneus s-IC as a hub because it was the component with the highest number of correlations with other identified s-ICs (frontal, cerebellar, parietal and motor areas in separated s-IC) in a healthy sample. In our study, all these brain areas are core and secondary regions of the L-FPN component, as described in other studies [16, 17, 18, 25, 102–105]. It is noteworthy that we extracted 20 components, while Segall et al. [87] extracted 70, which might explain the segregation in several components in their study compared to the regions identified in our s-IC2, as well as their pattern of correlations between segregated components. The regions involved in our L-FPN s-IC17 have been related with cognitive control [54] and associated with addiction in prior resting-state and task-related functional studies [4, 19, 66, 67]. In fact, studies that have analysed the effects of cocaine addiction have observed an increased functional recruitment of these networks (left FPN in particular) during drug-related processing, but a blunted response during nondrug-related processing [4, 16, 17, 19, 65]. In our study, the structural covariance between the brain structures making up the structural L-FPN is weakened in the CUD group compared to HCs. In this sense, it has been suggested that GM structural covariance networks mature after functional coactivation [87, 91], and the effects of neurodegenerative factors (e.g. cocaine addiction) could be a mechanism that explains how structural GM covariation occurs [87]. Therefore, our study suggests a significant reduction in the covariance within the regions of the L-FPN in the patients with CUD, which could reflect a maladaptive restructuring of these brain regions. This restructuring might be driven by factors that typically influence structural covariance during healthy development, such as age or functional connectivity.

The loading coefficient patterns of our structural L-FPN and the GMv of the CN revealed intriguing association patterns with other s-IC networks between groups. We identified a connection between the loading coefficient patterns of the structural L-FPN and other s-IC, specifically s-IC4, s-IC9 and s-IC16, as well as the GMv of the CN showed associations with s-IC11. Of these relations, the association between the L-FPN and s-IC16 was significant only in the HCs group, which indicates greater contribution in HCs compared to CUD. As one might expect, our structural networks do not precisely match the functional or resting-state networks described in previous studies [35, 87] and, therefore, we prefer to refer to them as s-IC. Notably, the core regions of our s-IC associated with our CN or L-FPN have been previously identified as altered in CUD in earlier network studies [4, 16, 17, 19]. The salience network, also known as the midcinguloinsular network (M-CIN), primarily comprises the anterior insula, dorsal anterior cingulate and inferior parietal lobe, regions involved in redirecting attentional resources toward salient stimuli. These regions are encompassed by our s-IC4 and have been observed to be altered in CUD [4, 25]. The amygdala and parahippocampus are the core regions of the limbic network, which has been observed to be less activated in CUD during emotional processing [19], and both regions are present in our s-IC9. However, these brain areas have been noted in some studies as additional regions of the M-CIN (see [25, 106, 107]). The thalamus and precuneus, which are key regions of the default mode network (DMN), have been also observed to be altered in CUD [4] and contribute to our s-IC11. However, these brain areas have been identified in some studies as additional regions of the L-FPN [25]. Lastly, in our s-IC16, we observed the angular gyrus in the superior parietal lobe extending into the intraparietal sulcus, the middle temporal gyrus and the frontal eye fields. These regions are key components of the dorsal frontoparietal network (D-FPN; [25]) and have also been described in other CUD studies [19, 62] to be linked with emotion regulation. We interpreted the association patterns uniquely observed in the HCs group, which are different from those in the CUD group, as indicative of a deviation from the typical developmental trajectory of structural brain networks potentially influenced or associated with cocaine use. Conversely, the specific association patterns identified in the CUD group may suggest a maladaptive restructuring tied to cocaine addiction. These interpretations become clearer when considering the core regions underlying each s-IC, as discussed. At a functional level, correlations between ICs are understood as the affiliation of a network (or a network subsystem) with other systems to collectively give rise to specific functions. For instance, various L-FPN subsystems have been delineated [25]. One of these subsystems shows a predominant connection to the regions in the D-FPN [108] and has been linked to the control of externally driven cognitive processes [109]. The functional affiliation between L-FPN and D-FPN seems to be reflected at the structural level in our study. In HCs, the loading coefficients of L-FPN were positively related to s-IC16 (which could be identified as a structural D-FPN, as explained above), while, interestingly, this link was not observed in CUD individuals. In turn, CUD was negatively related to s-IC4, which could be identified as a structural M-CIN (as explained), and also to s-IC9, which seems to encompass the additional areas described for M-CIN (see [25, 106, 107]). The core and additional functional M-CIN regions have been linked with salience domains [25]. Consequently, the patterns of association between s-IC suggest a neuroadaptation related to cocaine use. However, the relations based on the loading coefficients of GMc and volumetric patterns can be interpreted in different ways. As discussed earlier, the correlation of the L-FPN loading parameters with those of other s-ICs could indicate cocaine-induced degeneration of between-network connectivity. On the other hand, in the case of the CN, which exhibits greater consistency in CUD, the negative relation between the volume extracted from the network map and s-IC 11 (only in CUD) could suggest a disruption of structural growth related to a decrease in use or aberrant use [91] associated with cocaine use. By examining the primary structures that constitute these components and considering that the joint activation of different brain areas promotes their concurrent growth [24], we can better understand these relations. Our results suggest that (1) when the CN related to habit formation (due to the structures that it encompasses)

develops in CUD, the overall size of the primary DMN brain structures tends to reduce (because reduced brain structure use leads to less grey matter development; [24]) and (2) when a disturbance occurs in the normal L-FPN neurodevelopment (resulting in less consistency in CUD in factor loadings terms), the other networks involved in directing attention resources toward salient stimuli (salience) and, in both executive control and cognitive flexibility (D-FPN), may also be affected.

To the best of our knowledge, this is the first study that establishes a connection between cocaine use and abnormal structural covariance patterns. However, this pattern aligns with an expanding body of brain imaging research that emphasises the significant role of both brain region structures [3] and functional networks [4, 19] in the context of cocaine addiction.

Our study exhibits certain limitations that merit discussion. The lack of association with clinical and self-report variables despite differences in structural network loadings and volumes suggests a complex interplay between brain structure and clinical health. This may be due to limitations in clinical measurements (i.e. no control over other substances use in the CUD patient group or the potential presence of other behavioural addictions in both groups), long-term effects and the need to consider additional factors in future research. Furthermore, our study recruited samples with individual differences in clinical history terms, prioritising sample size over sample homogeneity. At this point, it is important to note that the FPN exhibits significant neuroanatomical variability among individuals [102, 110, 111], which could impact results concerning clinical and self-report variables. It is worth noting that exclusive cocaine use is challenging to find because polydrug use is the prevailing profile in addiction. To address this issue, we formulated our hypotheses based on the expectation of observing structural covariance patterns exclusively associated with the structures impacted by cocaine use, such as the supramarginal gyrus, left inferior parietal cortex and insula [58]. Therefore, the results should be cautiously interpreted. A secondary limitation of our study is that our findings are exclusive to males and, thus, cannot be generalised to females. Subsequent studies should be undertaken to explore the covariance patterns related to cocaine use in female populations.

5 | Conclusion

In summary, our study is the first to uncover structural covariance network alterations in individuals with CUD using the SBM approach. We identified significant differences in grey matter covariance loading coefficients in two key structural networks associated with various addiction-related deficits and cognitive control. The CN seems to constitute a neural network that evolves together with addictive processes. If we combine the results of our study with previous evidence, this network appears to be involved in the formation of consumption habits and the characteristic compulsion of addiction. Consequently, the development of this network in cocaine addiction could elucidate the difficulty to extinguish compulsive behaviours associated with consumption. The L-FPN, which is mainly composed of the brain structures responsible for contextual attention and signal integration, shows alterations in individuals with substance use. In this case, it seems to be predisposed to exclusive attention and an intensified interpretation of drug-related signals. Our study sheds light on the structural alterations in brain networks of individuals with CUD, and these findings provide a better understanding of cocaine addiction effects on both brain structure and network connectivity. Future research may consider combined structural and functional studies that include more clinical and addiction-related data to clarify the interpretation of the observed maladaptations.

Author Contributions

Elena Lacomba-Arnau: conceptualization, data analysis, and manuscript writing. Elena led the implementation of source-based morphometry techniques, performed statistical analyses, and contributed to the interpretation of results. **Agustín Martínez-Molina:** methodology supervision, data processing, and manuscript review. **Alfonso Barrós Loscertales:** conceptualization, data collection, analysis, manuscript writing, project supervision, funding acquisition, and critical manuscript review.

Acknowledgements

This publication is part of the PID2021-127340NB-C21 project, funded by MCIN/AEI/10.13039/501100011033/ERDF, EU. This work has been made possible thanks to the financial support of (a) the FI scholarship program of the Agència de Gestió d'Ajuts Universitaris i de Recerca de la Generalitat de Catalunya, through funding granted under the code '2023 FI-3 00107', and (b) the Universidad Autónoma de Madrid, through a researcher requalification grant (CA5/RSUE/2022-00133).

Conflicts of Interest

The authors declare no conflicts of interest.

Data Availability Statement

The data that support the findings of this study are available from the corresponding author upon reasonable request.

References

1. R. C. Pierce and L. J. Vanderschuren, "Kicking the Habit: The Neural Basis of Ingrained Behaviors in Cocaine Addiction," *Neuroscience & Biobehavioral Reviews* 35, no. 2 (2010): 212–219, https://doi.org/10.1016/j.neubiorev.2010.01.007.

2. A. Barrós-Loscertales, "Structural and Functional Aspects of Stimulant Misuse and Addiction," in *Neuropathology of Drug Addictions and Substance Misuse* (Academic Press, 2016), 209–219, https://doi.org/10.1016/B978-0-12-800212-4.00020-0.

3. V. Pando-Naude, S. Toxto, S. Fernandez-Lozano, C. E. Parsons, S. Alcauter, and E. A. Garza-Villarreal, "Gray and White Matter Morphology in Substance Use Disorders: A Neuroimaging Systematic Review and Meta-Analysis," *Translational Psychiatry* 11, no. 1 (2021): 29, https://doi.org/10.1038/s41398-020-01128-2.

4. A. Zilverstand, A. S. Huang, N. Alia-Klein, and R. Z. Goldstein, "Neuroimaging Impaired Response Inhibition and Salience Attribution in Human Drug Addiction: A Systematic Review," *Neuron* 98, no. 5 (2018): 886–903, https://doi.org/10.1016/j.neuron.2018.03.048.

5. A. Barrós-Loscertales, H. Garavan, J. C. Bustamante, et al., "Reduced Striatal Volume in Cocaine-Dependent Patients," *NeuroImage* 56, no. 3 (2011): 1021–1026, https://doi.org/10.1016/j.neuroimage.2011.02.035.

6. C. L. Crunelle, A. M. Kaag, H. E. Van den Munkhof, et al., "Dysfunctional Amygdala Activation and Connectivity With the Prefrontal Cortex in Current Cocaine Users," *Human Brain Mapping* 36, no. 10 (2015): 4222–4230, https://doi.org/10.1002/hbm.22913.

7. J. J. Prisciandaro, A. L. McRae-Clark, H. Myrick, S. Henderson, and K. T. Brady, "Brain Activation to Cocaine Cues and Motivation/Treatment Status," *Addiction Biology* 19, no. 2 (2014): 240–249, https://doi.org/10.1111/j.1369-1600.2012.00446.x.

8. M. E. Sim, I. K. Lyoo, C. C. Streeter, et al., "Cerebellar Gray Matter Volume Correlates With Duration of Cocaine Use in Cocaine-Dependent Subjects," *Neuropsychopharmacology* 32, no. 10 (2007): 2229–2237, https://doi.org/10.1038/sj.npp.1301346.

9. T. M. Le, S. Potvin, S. Zhornitsky, and C. S. R. Li, "Distinct Patterns of Prefrontal Cortical Disengagement During Inhibitory Control in Addiction: A Meta-Analysis Based on Population Characteristics," *Neuroscience & Biobehavioral Reviews* 127 (2021): 255–269.

10. H. Xu, C. Xu, and C. Guo, "Cocaine Use Disorder Is Associated With Widespread Surface-Based Alterations of the Basal Ganglia," *Journal of Psychiatric Research* 158 (2023): 95–103, https://doi.org/10.1016/j.jpsychires.2022.12.006.

11. L. Moreno-López, A. Catena, M. J. Fernández-Serrano, et al., "Trait Impulsivity and Prefrontal Gray Matter Reductions in Cocaine Dependent Individuals," *Drug and Alcohol Dependence* 125, no. 3 (2012): 208–214, https://doi.org/10.1016/j.drugalcdep.2012.02.012.

12. A. B. Konova, S. J. Moeller, and R. Z. Goldstein, "Common and Distinct Neural Targets of Treatment: Changing Brain Function in Substance Addiction," *Neuroscience & Biobehavioral Reviews* 37, no. 10 (2013): 2806–2817, https://doi.org/10.1016/j.neubiorev.2013.10.002.

13. R. Z. Goldstein and N. D. Volkow, "Drug Addiction and Its Underlying Neurobiological Basis: Neuroimaging Evidence for the Involvement of the Frontal Cortex," *American Journal of Psychiatry* 159, no. 10 (2002): 1642–1652, https://doi.org/10.1176/appi.ajp.159.10.1642.

14. T. E. Robinson and K. C. Berridge, "The Incentive Sensitization Theory of Addiction: Some Current Issues," *Philosophical Transactions of the Royal Society, B: Biological Sciences* 363, no. 1507 (2008): 3137–3146, https://doi.org/10.1098/rstb.2008.0093.

15. N. D. Volkow, G. J. Wang, J. S. Fowler, and D. Tomasi, "Addiction Circuitry in the Human Brain," *Annual Review of Pharmacology and Toxicology* 52, no. 1 (2012): 321–336.

16. V. Costumero and A. Barrós-Loscertales, "The Left Frontoparietal Brain Network in Addictions," in *Handbook of Substance Misuse and Addictions: From Biology to Public Health*, (Cham: Springer International Publishing, 2021): 1–24, https://doi.org/10.1007/978-3-030-67928-6_27-1.

17. V. Costumero, P. Rosell-Negre, J. C. Bustamante, et al., "Left Frontoparietal Network Activity Is Modulated by Drug Stimuli in Cocaine Addiction," *Brain Imaging and Behavior* 12 (2018): 1259–1270, https://doi.org/10.1007/s11682-017-9799-3.

18. J. Dang, Q. Tao, X. Niu, et al., "Meta-Analysis of Structural and Functional Brain Abnormalities in Cocaine Addiction," *Frontiers in Psychiatry* 13 (2022): 927075, https://doi.org/10.3389/fpsyt.2022.927075.

19. M. Picó-Pérez, V. Costumero, J. Verdejo-Román, et al., "Brain Networks Alterations in Cocaine Use and Gambling Disorders During Emotion Regulation," *Journal of Behavioral Addictions* 11 (2022): 373–385, https://doi.org/10.1556/2006.2022.00018.

20. K. D. Ersche, G. B. Williams, T. W. Robbins, and E. T. Bullmore, "Meta-Analysis of Structural Brain Abnormalities Associated With Stimulant Drug Dependence and Neuroimaging of Addiction Vulnerability and Resilience," *Current Opinion in Neurobiology* 23, no. 4 (2013): 615–624, https://doi.org/10.1016/j.conb.2013.02.017.

21. M. G. Hall, O. M. Alhassoon, M. J. Stern, et al., "Gray Matter Abnormalities in Cocaine Versus Methamphetamine-Dependent Patients: A Neuroimaging Meta-Analysis," *American Journal of Drug and Alcohol Abuse* 41, no. 4 (2015): 290–299, https://doi.org/10.3109/00952990.2015.1044607.

22. A. Alexander-Bloch, J. N. Giedd, and E. Bullmore, "Imaging Structural Co-Variance Between Human Brain Regions," *Nature Reviews Neuroscience* 14, no. 5 (2013): 322–336, https://doi.org/10.1038/nrn3465.

23. D. S. Bassett and M. S. Gazzaniga, "Understanding Complexity in the Human Brain," *Trends in Cognitive Sciences* 15, no. 5 (2011): 200–209, https://doi.org/10.1016/j.tics.2011.03.006.

24. E. Bullmore and O. Sporns, "Complex Brain Networks: Graph Theoretical Analysis of Structural and Functional Systems," *Nature Reviews Neuroscience* 10, no. 3 (2009): 186–198, https://doi.org/10.1038/nrn2575.

25. L. Q. Uddin, B. T. Yeo, and R. N. Spreng, "Towards a Universal Taxonomy of Macro-Scale Functional Human Brain Networks," *Brain Topography* 32, no. 6 (2019): 926–942, https://doi.org/10.1007/s10548-019-00744-6.

26. S. P. Burns, S. Santaniello, R. B. Yaffe, et al., "Network Dynamics of the Brain and Influence of the Epileptic Seizure Onset Zone," *Proceedings of the National Academy of Sciences* 111, no. 49 (2014): E5321–E5330, https://doi.org/10.1073/pnas.1401752111.

27. V. D. Calhoun, R. Miller, G. Pearlson, and T. Adalı, "The Chronnectome: Time-Varying Connectivity Networks as the Next Frontier in fMRI Data Discovery," *Neuron* 84, no. 2 (2014): 262–274, https://doi.org/10.1016/j.neuron.2014.10.015.

28. A. N. Khambhati, K. A. Davis, B. S. Oommen, et al., "Dynamic Network Drivers of Seizure Generation, Propagation and Termination in Human Neocortical Epilepsy," *PLoS Computational Biology* 11, no. 12 (2015): e1004608, https://doi.org/10.1371/journal.pcbi.1004608.

29. N. J. Kopell, H. J. Gritton, M. A. Whittington, and M. A. Kramer, "Beyond the Connectome: The Dynome," *Neuron* 83, no. 6 (2014): 1319–1328, https://doi.org/10.1016/j.neuron.2014.08.016.

30. S. Mizutaka and K. Yakubo, "Structural Instability of Large-Scale Functional Networks," *PLoS ONE* 12, no. 7 (2017): e0181247, https://doi.org/10.1371/journal.pone.0181247.

31. S. L. Mansour, Y. Tian, B. T. Yeo, V. Cropley, and A. Zalesky, "High-Resolution Connectomic Fingerprints: Mapping Neural Identity and Behavior," *NeuroImage* 229 (2021): 117695.

32. E. Dhamala, K. W. Jamison, A. Jaywant, S. Dennis, and A. Kuceyeski, "Distinct Functional and Structural Connections Predict Crystallised and Fluid Cognition in Healthy Adults," *Human Brain Mapping* 42, no. 10 (2021): 3102–3118, https://doi.org/10.1002/hbm.25420.

33. A. J. Holmes, M. O. Hollinshead, T. M. O'keefe, et al., "Brain Genomics Superstruct Project Initial Data Release With Structural, Functional, and Behavioral Measures," *Scientific Data* 2, no. 1 (2015): 1–16, https://doi.org/10.1038/sdata.2015.31.

34. L. Q. R. Ooi, J. Chen, S. Zhang, et al., "Comparison of Individualized Behavioral Predictions Across Anatomical, Diffusion and Functional Connectivity MRI," *NeuroImage* 263 (2022): 119636, https://doi.org/10.1016/j.neuroimage.2022.119636.

35. C. N. Gupta, J. A. Turner, and V. D. Calhoun, "Source-Based Morphometry: A Decade of Covarying Structural Brain Patterns," *Brain Structure and Function* 224, no. 9 (2019): 3031–3044, https://doi.org/10.1007/s00429-019-01969-8.

36. J. Ashburner and K. J. Friston, "Voxel-Based Morphometry—The Methods," *NeuroImage* 11, no. 6 (2000): 805–821, https://doi.org/10.1006/nimg.2000.0582.

37. M. J. McKeown and T. J. Sejnowski, "Independent Component Analysis of fMRI Data: Examining the Assumptions," *Human Brain Mapping* 6, no. 5–6 (1998): 368–372, https://doi.org/10.1002/(SICI)1097-0193(1998)6:5/6<368::AID-HBM7>3.0.CO;2-E.

38. L. Xu, K. M. Groth, G. Pearlson, D. J. Schretlen, and V. D. Calhoun, "Source-Based Morphometry: The Use of Independent Component Analysis to Identify Gray Matter Differences With Application to Schizophrenia," *Human Brain Mapping* 30, no. 3 (2009a): 711–724, https://doi.org/10.1002/hbm.20540.

39. A. Caprihan, C. Abbott, J. Yamamoto, et al., "Source-Based Morphometry Analysis of Group Differences in Fractional Anisotropy in Schizophrenia," *Brain Connectivity* 1, no. 2 (2011): 133–145, https://doi.org/10.1089/brain.2011.0015.

40. L. Xu, G. Pearlson, and V. D. Calhoun, "Joint Source Based Morphometry Identifies Linked Gray and White Matter Group Differences," *NeuroImage* 44, no. 3 (2009b): 777–789, https://doi.org/10.1016/j.neuroimage.2008.09.051.

41. G. D. Pearlson, "Etiologic, Phenomenologic, and Endophenotypic Overlap of Schizophrenia and Bipolar Disorder," *Annual Review of Clinical Psychology* 11 (2015): 251–281, https://doi.org/10.1146/annurev-clinpsy-032814-112915.

42. J. Sui, T. Adali, Q. Yu, J. Chen, and V. D. Calhoun, "A Review of Multivariate Methods for Multimodal Fusion of Brain Imaging Data," *Journal of Neuroscience Methods* 204, no. 1 (2012): 68–81, https://doi.org/10.1016/j.jneumeth.2011.10.031.

43. A. C. Evans, "Networks of Anatomical Covariance," *NeuroImage* 80 (2013): 489–504, https://doi.org/10.1016/j.neuroimage.2013.05.054.

44. E. Castro, R. D. Hjelm, S. M. Plis, L. Dinh, J. A. Turner, and V. D. Calhoun, "Deep Independence Network Analysis of Structural Brain Imaging: Application to Schizophrenia," *IEEE Transactions on Medical Imaging* 35, no. 7 (2016): 1729–1740, https://doi.org/10.1109/TMI.2016.2527717.

45. M. Ke, F. Wang, and G. Liu, "Altered Effective Connectivity of the Default Mode Network in Juvenile Myoclonic Epilepsy," *Cognitive Neurodynamics* 18 (2024): 1549–1561, https://doi.org/10.1007/s11571-023-09994-4.

46. G. Lapomarda, A. Grecucci, I. Messina, E. Pappaianni, and H. Dadomo, "Common and Different Gray and White Matter Alterations in Bipolar and Borderline Personality Disorder: A Source-Based Morphometry Study," *Brain Research* 1762 (2021a): 147401, https://doi.org/10.1016/j.brainres.2021.147401.

47. G. Lapomarda, E. Pappaianni, R. Siugzdaite, A. G. Sanfey, R. I. Rumiati, and A. Grecucci, "Out of Control: An Altered Parieto-Occipital-Cerebellar Network for Impulsivity in Bipolar Disorder," *Behavioural Brain Research* 406 (2021b): 113228, https://doi.org/10.1016/j.bbr.2021.113228.

48. C. N. Gupta, V. D. Calhoun, S. Rachakonda, et al., "Patterns of Gray Matter Abnormalities in Schizophrenia Based on an International Mega-Analysis," *Schizophrenia Bulletin* 41, no. 5 (2015): 1133–1142, https://doi.org/10.1093/schbul/sbu177.

49. M. Li, W. Deng, Y. Li, et al., "Ameliorative Patterns of Grey Matter in Patients With First-Episode and Treatment-Naïve Schizophrenia," *Psychological Medicine* 53, no. 8 (2023): 3500–3510, https://doi.org/10.1017/S0033291722000058.

50. S. Sorella, G. Lapomarda, I. Messina, et al., "Testing the Expanded Continuum Hypothesis of Schizophrenia and Bipolar Disorder. Neural and Psychological Evidence for Shared and Distinct Mechanisms," *NeuroImage: Clinical* 23 (2019): 101854, https://doi.org/10.1016/j.nicl.2019.101854.

51. A. Grecucci, D. Rubicondo, R. Siugzdaite, L. Surian, and R. Job, "Uncovering the Social Deficits in the Autistic Brain. A Source-Based Morphometric Study," *Frontiers in Neuroscience* 10 (2016): 388, https://doi.org/10.3389/fnins.2016.00388.

52. E. Premi, V. D. Calhoun, V. Garibotto, et al., "Source-Based Morphometry Multivariate Approach to Analyze [123 I] FP-CIT SPECT Imaging," *Molecular Imaging and Biology* 19 (2017): 772–778, https://doi.org/10.1007/s11307-017-1052-3.

53. T. Samantaray, J. Saini, P. K. Pal, and C. N. Gupta, "Brain Connectivity for Subtypes of Parkinson's Disease Using Structural MRI," *Biomedical Physics & Engineering Express* 10, no. 2 (2024): 025012, https://doi.org/10.1088/2057-1976/ad1e77.

54. N. Bergsland, D. Horakova, M. G. Dwyer, et al., "Gray Matter Atrophy Patterns in Multiple Sclerosis: A 10-Year Source-Based Morphometry Study," *NeuroImage: Clinical* 17 (2018): 444–451, https://doi.org/10.1016/j.nicl.2017.11.002.

55. J. A. Ciarochi, V. D. Calhoun, S. Lourens, et al., "Patterns of Co-Occurring Gray Matter Concentration Loss Across the Huntington Disease Prodrome," *Frontiers in Neurology* 7 (2016): 147, https://doi.org/10.3389/fneur.2016.00147.

56. K. A. Kiehl, N. E. Anderson, E. Aharoni, et al., "Age of Gray Matters: Neuroprediction of Recidivism," *NeuroImage: Clinical* 19 (2018): 813–823, https://doi.org/10.1016/j.nicl.2018.05.03.

57. K. Al-Khalil, R. P. Bell, S. L. Towe, S. Gadde, E. Burke, and C. S. Meade, "Cortico-Striatal Networking Deficits Associated With Advanced HIV Disease and Cocaine use," *Journal of Neurovirology* 29, no. 2 (2023): 167–179, https://doi.org/10.1007/s13365-023-01120-8.

58. S. Mackey, N. Allgaier, B. Chaarani, et al., "Mega-Analysis of Gray Matter Volume in Substance Dependence: General and Substance-Specific Regional Effects," *American Journal of Psychiatry* 176, no. 2 (2019): 119–128, https://doi.org/10.1176/appi.ajp.2018.17040415.

59. A. M. L. Bittencourt, V. F. Bampi, R. C. Sommer, et al., "Cortical Thickness and Subcortical Volume Abnormalities in Male Crack-Cocaine Users," *Psychiatry Research: Neuroimaging* 310 (2021): 111232, https://doi.org/10.1016/j.pscychresns.2020.111232.

60. L. Vaquero, E. Cámara, F. Sampedro, et al., "Cocaine Addiction Is Associated With Abnormal Prefrontal Function, Increased Striatal Connectivity and Sensitivity to Monetary Incentives, and Decreased Connectivity Outside the Human Reward Circuit," *Addiction Biology* 22, no. 3 (2017): 844–856, https://doi.org/10.1111/adb.12356.

61. S. Mackey and M. Paulus, "Are There Volumetric Brain Differences Associated With the Use of Cocaine and Amphetamine-Type Stimulants?," *Neuroscience & Biobehavioral Reviews* 37, no. 3 (2013): 300–316, https://doi.org/10.1016/j.neubiorev.2012.12.003.

62. J. T. Buhle, J. A. Silvers, T. D. Wager, et al., "Cognitive Reappraisal of Emotion: A Meta-Analysis of Human Neuroimaging Studies," *Cerebral Cortex* 24, no. 11 (2014): 2981–2990, https://doi.org/10.1093/cercor/bht154.

63. J. C. Bustamante, A. Barrós-Loscertales, V. Costumero, et al., "Abstinence Duration Modulates Striatal Functioning During Monetary Reward Processing in Cocaine Patients," *Addiction Biology* 19, no. 5 (2014): 885–894, https://doi.org/10.1111/adb.12041.

64. K. D. Ersche, A. Barnes, P. S. Jones, S. Morein-Zamir, T. W. Robbins, and E. T. Bullmore, "Abnormal Structure of Frontostriatal Brain Systems Is Associated With Aspects of Impulsivity and Compulsivity in Cocaine Dependence," *Brain* 134, no. 7 (2011): 2013–2024, https://doi.org/10.1093/brain/awr138.

65. A. Barrós-Loscertales, V. Costumero, P. Rosell-Negre, P. Fuentes-Claramonte, J. J. Llopis-Llacer, and J. C. Bustamante, "Motivational Factors Modulate Left Frontoparietal Network During Cognitive Control in Cocaine Addiction," *Addiction Biology* 25, no. 4 (2020): e12820, https://doi.org/10.1111/adb.12820.

66. R. Z. Goldstein and N. D. Volkow, "Dysfunction of the Prefrontal Cortex in Addiction: Neuroimaging Findings and Clinical Implications," *Nature Reviews Neuroscience* 12, no. 11 (2011): 652–669, https://doi.org/10.1038/nrn3119.

67. A. Zilverstand, M. A. Parvaz, and R. Z. Goldstein, "Neuroimaging Cognitive Reappraisal in Clinical Populations to Define Neural Targets for Enhancing Emotion Regulation. A Systematic Review," *NeuroImage* 151 (2017): 105–116, https://doi.org/10.1016/j.neuroimage.2016.06.009.

68. A. Zilverstand, M. A. Parvaz, S. J. Moeller, and R. Z. Goldstein, "Cognitive Interventions for Addiction Medicine: Understanding the Underlying Neurobiological Mechanisms," *Progress in Brain Research* 224 (2016): 285–304, https://doi.org/10.1016/bs.pbr.2015.07.019.

69. M. P. Bryden, "Measuring Handedness With Questionnaires," *Neuropsychologia* 15, no. 4–5 (1977): 617–624, https://doi.org/10.1016/0028-3932(77)90067-7.

70. R. C. Oldfield, "The Assessment and Analysis of Handedness: The Edinburgh Inventory," *Neuropsychologia* 9, no. 1 (1971): 97–113, https://doi.org/10.1016/0028-3932(71)90067-4.

71. F. González-Sáiz, A. Domingo-Salvany, G. Barrio, et al., "Severity of Dependence Scale as a Diagnostic Tool for Heroin and Cocaine Dependence," *European Addiction Research* 15, no. 2 (2009): 87–93, https://doi.org/10.1159/000189787.

72. K. M. Kampman, J. R. Volpicelli, D. E. Mcginnis, et al., "Reliability and Validity of the Cocaine Selective Severity Assessment," *Addictive Behaviors* 23, no. 4 (1998): 449–461, https://doi.org/10.1016/S0306-4603(98)00011-2.

73. S. T. Tiffany, E. Singleton, C. A. Haertzen, and J. E. Henningfield, "The Development of a Cocaine Craving Questionnaire," *Drug and Alcohol Dependence* 34, no. 1 (1993): 19–28, https://doi.org/10.1016/0376-8716(93)90042-O.

74. University of Jena, Department of Neurology, "CAT - A Computational Anatomy Toolbox for the Analysis of Structural MRI Data," (n.d.), http://www.neuro.uni-jena.de/cat/.

75. A. Fornito, M. Yücel, J. Patti, S. J. Wood, and C. Pantelis, "Mapping Grey Matter Reductions in Schizophrenia: An Anatomical Likelihood Estimation Analysis of Voxel-Based Morphometry Studies," *Schizophrenia Research* 108, no. 1–3 (2009): 104–113, https://doi.org/10.1016/j.schres.2008.12.011.

76. S. A. Meda, N. R. Giuliani, V. D. Calhoun, et al., "A Large Scale (N= 400) Investigation of Gray Matter Differences in Schizophrenia Using Optimized Voxel-Based Morphometry," *Schizophrenia Research* 101, no. 1–3 (2008): 95–105, https://doi.org/10.1016/j.schres.2008.02.007.

77. M. R. Arbabshirani, S. Plis, J. Sui, and V. D. Calhoun, "Single Subject Prediction of Brain Disorders in Neuroimaging: Promises and Pitfalls," *NeuroImage* 145 (2017): 137–165, https://doi.org/10.1016/j.neuroimage.2016.02.07.

78. Gift of the Gab, "Group ICA of fMRI Toolbox (GIFT)," (n.d.), http://icatb.sourceforge.net.

79. A. J. Bell and T. J. Sejnowski, "An Information-Maximization Approach to Blind Separation and Blind Deconvolution," *Neural Computation* 7, no. 6 (1995): 1129–1159, https://doi.org/10.1162/neco.1995.7.6.1129.

80. T. W. Lee, M. Girolami, and T. J. Sejnowski, "Independent Component Analysis Using an Extended Infomax Algorithm for Mixed Subgaussian and Supergaussian Sources," *Neural Computation* 11, no. 2 (1999): 417–441, https://doi.org/10.1162/089976699300016719.

81. University, "ICASSO: Software for Investigating the Reliability of ICA Estimates by Clustering and Visualization," (n.d.), http://research.ics.aalto.fi/ica/icasso/.

82. E. Pappaianni, R. Siugzdaite, S. Vettori, P. Venuti, R. Job, and A. Grecucci, "Three Shades of Grey: Detecting Brain Abnormalities in Children With Autism Using Source-, Voxel-and Surface-Based Morphometry," *European Journal of Neuroscience* 47, no. 6 (2017): 690–700, https://doi.org/10.1111/ejn.13704.

83. Research Imaging Institute, UT Health San Antonio, "Mango," (n.d.), http://ric.uthscsa.edu/mango/Aalto.

84. N. Canessa, C. Crespi, M. Motterlini, et al., "The Functional and Structural Neural Basis of Individual Differences in Loss Aversion," *Journal of Neuroscience* 33, no. 36 (2013): 14307–14317, https://doi.org/10.1523/JNEUROSCI.0497-13.2013.

85. M. S. Depping, N. D. Wolf, N. Vasic, F. Sambataro, P. A. Thomann, and R. C. Wolf, "Common and Distinct Structural Network Abnormalities in Major Depressive Disorder and Borderline Personality Disorder," *Progress in Neuro-Psychopharmacology and Biological Psychiatry* 65 (2016): 127–133, https://doi.org/10.1016/j.pnpbp.2015.09.007.

86. C. R. Genovese, N. A. Lazar, and T. Nichols, "Thresholding of Statistical Maps in Functional Neuroimaging Using the False Discovery Rate," *NeuroImage* 15, no. 4 (2002): 870–878, https://doi.org/10.1006/nimg.2001.1037.

87. J. M. Segall, E. A. Allen, R. E. Jung, et al., "Correspondence Between Structure and Function in the Human Brain at Rest," *Frontiers in Neuroinformatics* 6 (2012): 10, https://doi.org/10.3389/fninf.2012.00010.

88. G. Ridgway, "VBM8 Toolbox," (n.d.), http://www0.cs.ucl.ac.uk/staff/g.ridgway/vbm/get_totals.m.

89. J. Adrián-Ventura, V. Costumero, M. A. Parcet, and C. Ávila, "Linking Personality and Brain Anatomy: A Structural MRI Approach to Reinforcement Sensitivity Theory," *Social Cognitive and Affective Neuroscience* 14, no. 3 (2019): 329–338, https://doi.org/10.1093/scan/nsz011.

90. IBM, "SPSS Statistics Software," (n.d.), https://www.ibm.com/analytics/spss-statistics-software.

91. B. A. Zielinski, E. D. Gennatas, J. Zhou, and W. W. Seeley, "Network-Level Structural Covariance in the Developing Brain," *Proceedings of the National Academy of Sciences* 107, no. 42 (2010): 18191–18196.

92. A. Kübler, K. Murphy, and H. Garavan, "Cocaine Dependence and Attention Switching Within and Between Verbal and Visuospatial Working Memory," *European Journal of Neuroscience* 21, no. 7 (2005): 1984–1992, https://doi.org/10.1111/j.1460-9568.2005.04027.x.

93. L. Moreno-López, J. C. Perales, D. van Son, et al., "Cocaine Use Severity and Cerebellar Gray Matter Are Associated With Reversal Learning Deficits in Cocaine-Dependent Individuals," *Addiction Biology* 20, no. 3 (2015): 546–556, https://doi.org/10.1111/adb.12143.

94. E. A. Moulton, I. Elman, L. R. Becerra, R. Z. Goldstein, and D. Borsook, "The Cerebellum and Addiction: Insights Gained From Neuroimaging Research," *Addiction Biology* 19, no. 3 (2014): 317–331, https://doi.org/10.1111/adb.12101.

95. J. L. Aron and M. P. Paulus, "Location, Location: Using Functional Magnetic Resonance Imaging to Pinpoint Brain Differences Relevant to Stimulant Use," *Addiction* 102 (2007): 33–43, https://doi.org/10.1111/j.1360-0443.2006.01778.x.

96. J. C. Bustamante, A. Barrós-Loscertales, N. Ventura-Campos, et al., "Right Parietal Hypoactivation in a Cocaine-Dependent Group During a Verbal Working Memory Task," *Brain Research* 1375 (2011): 111–119, https://doi.org/10.1016/j.brainres.2010.12.042.

97. H. Garavan, J. N. Kaufman, and R. Hester, "Acute Effects of Cocaine on the Neurobiology of Cognitive Control," *Philosophical Transactions of the Royal Society, B: Biological Sciences* 363, no. 1507 (2008): 3267–3276, https://doi.org/10.1098/rstb.2008.0106.

98. S. D. Lane, J. L. Steinberg, L. Ma, et al., "Diffusion Tensor Imaging and Decision Making in Cocaine Dependence," *PLoS ONE* 5, no. 7 (2010): e11591, https://doi.org/10.1371/journal.pone.0011591.

99. D. Tomasi, L. Chang, E. C. Caparelli, and T. Ernst, "Different Activation Patterns for Working Memory Load and Visual Attention Load," *Brain Research* 1132 (2007): 158–165, https://doi.org/10.1016/j.brainres.2006.11.030.

100. H. Gu, B. J. Salmeron, T. J. Ross, et al., "Mesocorticolimbic Circuits Are Impaired in Chronic Cocaine Users as Demonstrated by Resting-State Functional Connectivity," *NeuroImage* 53, no. 2 (2010): 593–601, https://doi.org/10.1016/j.neuroimage.2010.06.066.

101. M. J. McHugh, C. H. Demers, B. J. Salmeron, M. D. Devous, Sr., E. A. Stein, and B. Adinoff, "Cortico-Amygdala Coupling as a Marker of Early Relapse Risk in Cocaine-Addicted Individuals," *Frontiers in Psychiatry* 5 (2014): 16, https://doi.org/10.3389/fpsyt.2014.00016.

102. E. M. Gordon, T. O. Laumann, A. W. Gilmore, et al., "Precision Functional Mapping of Individual Human Brains," *Neuron* 95, no. 4 (2017): 791–807, https://doi.org/10.1016/j.neuron.2017.07.011.

103. T. A. Niendam, A. R. Laird, K. L. Ray, Y. M. Dean, D. C. Glahn, and C. S. Carter, "Meta-Analytic Evidence for a Superordinate Cognitive Control Network Subserving Diverse Executive Functions," *Cognitive, Affective, & Behavioral Neuroscience* 12 (2012): 241–268, https://doi.org/10.3758/s13415-011-0083-5.

104. S. M. Smith, P. T. Fox, K. L. Miller, et al., "Correspondence of the Brain's Functional Architecture During Activation and Rest," *Proceedings of the National Academy of Sciences* 106, no. 31 (2009): 13040–13045, https://doi.org/10.1073/pnas.090526710.

105. B. T. Yeo, F. M. Krienen, J. Sepulcre, et al., "The Organization of the Human Cerebral Cortex Estimated by Intrinsic Functional Connectivity," *Journal of Neurophysiology* 106 (2011): 1125–1165, https://doi.org/10.1152/jn.00338.2011.

106. W. W. Seeley, V. Menon, A. F. Schatzberg, et al., "Dissociable Intrinsic Connectivity Networks for Salience Processing and Executive Control," *Journal of Neuroscience* 27, no. 9 (2007): 2349–2356, https://doi.org/10.1523/JNEUROSCI.5587-06.2007.

107. L. Q. Uddin, "Salience Processing and Insular Cortical Function and Dysfunction," *Nature Reviews Neuroscience* 16, no. 1 (2015): 55–61, https://doi.org/10.1038/nrn3857.

108. M. L. Dixon, A. De La Vega, C. Mills, et al., "Heterogeneity Within the Frontoparietal Control Network and Its Relationship to the Default and Dorsal Attention Networks," *Proceedings of the National Academy of Sciences* 115, no. 7 (2018): E1598–E1607, https://doi.org/10.1073/pnas.1715766115.

109. A. C. Murphy, M. A. Bertolero, L. Papadopoulos, D. M. Lydon-Staley, and D. S. Bassett, "Multimodal Network Dynamics Underpinning Working Memory," *Nature Communications* 11, no. 1 (2020): 3035, https://doi.org/10.1038/s41467-020-15541-0.

110. S. Marek and N. U. Dosenbach, "The Frontoparietal Network: Function, Electrophysiology, and Importance of Individual Precision Mapping," *Dialogues in Clinical Neuroscience* 20, no. 2 (2018): 133–140.

111. S. Mueller, D. Wang, M. D. Fox, et al., "Individual Variability in Functional Connectivity Architecture of the Human Brain," *Neuron* 77, no. 3 (2013): 586–595, https://doi.org/10.1016/j.neuron.2012.12.028.

Supporting Information

Additional supporting information can be found online in the Supporting Information section.